ACS APPLIED MATERIALS & INTERFACES

Research Article

www.acsami.org

Photocatalytic Degradation of Methyl Orange Using a TiO_2/Ti Mesh Electrode with 3D Nanotube Arrays

Jianjun Liao, Shiwei Lin,* Li Zhang, NengQian Pan, Xiankun Cao, and Jianbao Li

Key Laboratory of Ministry of Education for Application Technology of Chemical Materials in Hainan Superior Resources, School of Materials and Chemical Engineering, Hainan University, Haikou 570228, Hainan, People's Republic of China

Supporting Information

ABSTRACT: To further improve the photocatalytic techniques for water purification and wastewater treatment, we successfully prepared a new type of TiO_2/Ti mesh photoelectrode, by anodization in ethylene glycol solution. The three-dimensional arrays of nanotubes formed on Ti mesh show a significant improvement in photocatalytic activity, compared to the nanotube arrays formed on foil. This can be demonstrated by about 22 and 38% enhancement in the degradation efficiency per mass and per area, respectively, when TiO_2/Ti mesh electrode was used to photocatalyze methyl orange (MO). Furthermore, the effects of different parameters on MO photodegradation were investigated, such as different photoelectrode calcination temperature, the initial pH value of MO solution, and the present of hydrogen peroxide. The superior photocatalytic activity could be achieved by the TiO_2/Ti mesh photoelectrode calcinated at 550 °C, due to the appearance of mixed crystal phases of anatase and rutile. In strong acidic or caustic conditions, such as pH 1 or 13, a high degradation efficiency can be both obtained. The presence of H_2O_2 in photocatalytic reactions can promote photocatalytic degradation efficiencies. Moreover, the experimental results demonstrated the excellent stability and reliability of the TiO_2/Ti mesh electrode.

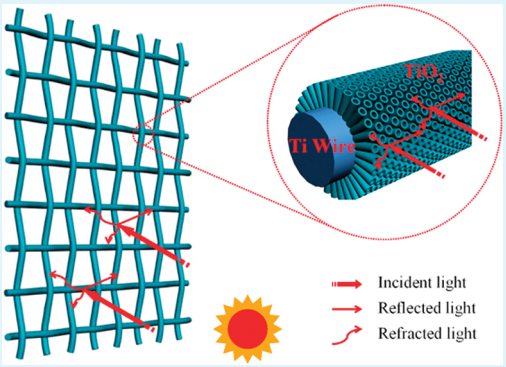

KEYWORDS: *Ti mesh, TiO_2, 3D, nanotube, photocatalytic activity*

1. INTRODUCTION

The efficient treatment of industrial wastewaters and contaminated drinking water sources has become of great importance in a world that is facing with ever increasing population and decreasing energy resources.[1] However, the use of conventional water and wastewater treatment processes becomes increasingly challenged with the identification of more and more contaminants, rapid growth of population and industrial activities, and diminishing availability of water resources.[2] In recent years, semiconductor photocatalytic process has shown a great potential as a low-cost, environmentally friendly, and sustainable treatment technology to align with the "zero" waste scheme in the water/wastewater industry.[3] This advanced oxidation technology is characterized by a common chemical action, which basically relies on the primary reactivity of OH radicals in driving oxidation processes, ultimately resulting in the mineralization of a variety of environmental pollutants.[4−7]

Among the plentiful semiconductor catalysts, TiO_2 photocatalysts are one type of attractive and promising materials due to their excellent properties such as a high photocatalytic activity, stability, and nontoxicity. TiO_2 can be used as a powder or as a film for photocatalytic degradation. If the TiO_2 is used in a suspension reactor, highly dispersed TiO_2 powder must be removed following the treatment. Post-treatment removal requires a solid−liquid separation stage which adds to the overall capital and running costs of the plant.[8] The immobilization of TiO_2 as a film on a suitable substrate can minimize post-treatment. Many efforts were trying to immobilize TiO_2 particles as a film by a simple sol−gel process.[9−11] Unfortunately, because of its relatively low specific surface area, the photocatalytic activity is limited.

The newly developed TiO_2 nanotube arrays show great advantages on preparing an immobilized photocatalytic electrode. Compared with a particulate film, TiO_2 nanotube arrays possess larger surface area, faster electron transport and lower recombination rate, enabling us to achieve a higher photocatalytic activity and efficiency. However, the use of Ti in the form of a foil can be expensive and wasteful. For instance, Grimes et al. found that only about 2% weight of the titanium was converted into nanotubes and the underlying barrier layer after anodization in HF aqueous solution.[12] Recent studies found that TiO_2 nanotube arrays of 1.0 mm length could be obtained upon anodizing 1.0 mm thick Ti foil in organic electrolyte.[13] This means that Ti foil could be completely converted into nanotubes, and the utilization efficiency is nearly 100%. However, nanotubes with a few micrometers thickness are enough to perform efficient photocatalysis. The further

Received: September 9, 2011
Accepted: November 25, 2011
Published: November 25, 2011

increasing nantubes thickness is not helpful for the photocatalytic activity, and the photocatalytic activity would even decrease instead.[14,15] One option to avoid this wastage is the formation of TiO_2 nanotubes on Ti mesh. Unlike planar Ti foil where tubes are grown vertically in two-dimensional (2D) arrays, the TiO_2/Ti mesh photoelectrode consists of tubes that extend radically in three-dimensional (3D) arrays from a grid of fine titanium wires.[16] Therefore, loss of photons attributed to scattering effects in the liquid can potentially be minimized because the nanotubes can absorb reflected and/or refracted light.[17] Further, it is expected that the photocatalytic activity might be enhanced compared to the nanotubes formed on foils.

In this study, a TiO_2/Ti mesh electrode as a new type of photoelectrode was produced by fabricating TiO_2 nanotube arrays on Ti mesh using an anodization process, and methyl orange (MO) was used as a model compound for photocatalytic activity study under UV irradiation. Photocatalytic activities of nanotubes formed on both Ti foil and mesh were compared, and a significantly enhanced photocatalytic activity of TiO_2/Ti mesh electrode was demonstrated. Furthermore, the effects of different parameters such as different calcination temperature, initial solution pH and the present of hydrogen peroxide on MO photodegradation were investigated. Experiments were also performed to investigate the reliability and stability of the TiO_2/Ti mesh electrode.

2. EXPERIMENTAL SECTION

2.1. Preparation of TiO_2/Ti Mesh Electrode. A large piece of raw Ti mesh with thickness of 0.4 mm was cut into small square pieces of 20 × 20 mm^2, which were then cleaned with acetone, ethanol and deionized water, respectively. Anodization was performed in a two-electrode configuration with titanium mesh as the working electrode and stainless steel foil as the counter electrode. The interval between the working and counter electrodes was about 3 cm. A direct current power supply was used as the voltage source to drive the anodization. The electrolyte consisted of 0.3 wt % NH_4F and 2 vol % H_2O in ethylene glycol. The Ti mesh was anodized at 60 V for 3 h at room temperature. After anodization, the samples were annealed at different temperatures (350, 450, and 550 °C) for 3 h in the air. For a comparison, a TiO_2/Ti foil electrode with the same size as the Ti mesh was also prepared at the same conditions.

2.2. Characterization of TiO_2/Ti Mesh Electrode. The morphology and crystal structure of TiO_2/Ti mesh electrode was characterized by field-emission scanning electronic microscopy (FESEM, Hitachi S4800, Japan), polarizing microscope (Leica DMRX, Germany), and X-ray diffraction technique (XRD, Bruker D8, Germany), respectively.

2.3. Photocurrent Measurement. Photocurrent was measured using an electrochemical workstation (Zanher zennium, Germany) in a three-electrode configuration with a Pt wire counter electrode and a saturated calomel reference electrode. The working electrode, including TiO_2/Ti mesh and TiO_2/Ti foil, was illuminated with UV light (370.8 nm, 0.3 mW/cm^2 illumination on the photoanode). A 1 M KOH aqueous solution was used as the electrolyte.

2.4. Photocatalytic Degradation of Methyl Orange. Methyl orange was used as a model compound to monitor the photocatalytic activity of the TiO_2/Ti mesh electrode. Before experiments started, the MO solution with photoelectrode inside was left in a dark environment for 30 min to achieve adsorption/desorption equilibrium. And then it was irradiated by using a 300 W high-pressure mercury lamp with a strongest wavelength of 365 nm (Shanghai Bilon Instruments Co., Ltd., GGZ300), which was surrounded by a quartz cooling thimble. The lamp was placed at the top of the reactor with the spacing between the light bulb and the surface of electrodes being 5 cm. The pH value of MO solution was adjusted with 1 M H_2SO_4 or 1 M NaOH to the desired values in order to study the influence of pH value on MO degradation. To investigate the effect of presence of hydrogen peroxide, we added 0.3 mM H_2O_2 to MO solution. Without special mention, all the TiO_2/Ti mesh and TiO_2/Ti foil electrodes were annealed at 450 °C, and the pH value was fixed at natural pH (pH 7), and no H_2O_2 was added into MO solution during photodegradation reaction. The initial concentration of MO solution was 5 mg/L (indicated by the initial absorbance and denoted as C_0), and the concentration of MO during reaction (denoted as C) was monitored by a UV−vis spectrophotometer (TU-1901, Purkinje, China). The MO degradation efficiency was usually determined using the following eq 1. Besides the degradation time, the degradation efficiency is strongly associated with the amount of the photocatalytic materials used in the experiment. Thus the degradation efficiency per mass or per area was further defined as degradation efficiency divided by the mass or surface area of the electrodes exposed to illumination, respectively.

$$\text{degradation efficiency } (\%) = \frac{C_0 - C}{C_0} 100 \quad (1)$$

3. RESULTS AND DISCUSSION

3.1. Characteristics of TiO_2/Ti Mesh Electrodes. Figure 1a shows the digital image of Ti mesh before and after anodization. The color of Ti mesh changes from silver to dark color, indicating that a TiO_2 nanotube layer was formed on the mesh surface. Restricted by the mismatch between SEM's resolution and Ti wire's diameter, a panoramic display that outer TiO_2 naotube arrays are radially grown on the Ti wire could not be properly presented. Thus, an optical microscope like polarizing microscope was chosen to characterize the anodized Ti wire. As shown in Figure 1b, TiO_2 nanotube bundles are interspaced with several fissures at irregular intervals, unlike nanotubes grown on Ti foils where such fissures are absent. This can be attributed to van der Waals attraction and capillary forces during drying.[18] Figure 1c depicts that TiO_2 nanotube arrays are vertical to the Ti wire substrate. Unlike planar Ti foil where tubes are grown vertically in 2D arrays, TiO_2 nanotube arrays grown on Ti wires are radially extended in 3D arrays. The schematic diagrams of the photoelectrodes composed of 3D and 2D nanotube arrays are

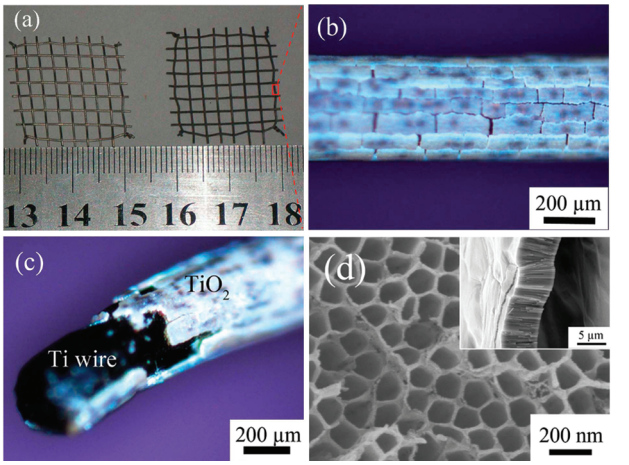

Figure 1. Morphology characterization of the TiO_2/Ti mesh electrode: (a) digital image of TiO_2/Ti mesh electrode before (left) and after (right) anodization. (b) Magnified image of red marked region of (a) using polarizing microscope. (c) Polarizing microscope image of an anodized Ti wire, in which outer TiO_2 nanotube array was partially peeled off. (d) SEM image of top view of TiO_2 nanotube array, and the inset shows the cross-sectional view.

shown in Figure S1 in the Supporting Information. On the basis of such 3D configured nanotubes, it could be expected that such a 3D mesh might possess a more excellent photocatalytic activity than a 2D foil, which will be discussed later. As shown in Figure 1d, the nanotubes grown on Ti mesh have an average diameter 150 nm and an average length of 5 μm. The diameter is consistent with the dimension of nanotubes grown on planar titanium foil under the identical anodization conditions, while the length is smaller than that of the nanotubes grown on Ti foil, where the tube length is 7 μm (see Figure S2 in the Supporting Information). Meanwhile, it can be seen from the inset of Figure 1d that the interface between TiO_2 nanotube arrays and Ti wire substrate seems to be separated, which might cause by the stress when Ti wire was cut down during the SEM characterization. While, in fact, the nanotubes grown on Ti wire are stable and adhesive because of the support from the adjacent tubes.

Figure 2 shows the XRD patterns of TiO_2/Ti mesh electrodes calcined at different temperatures. When the

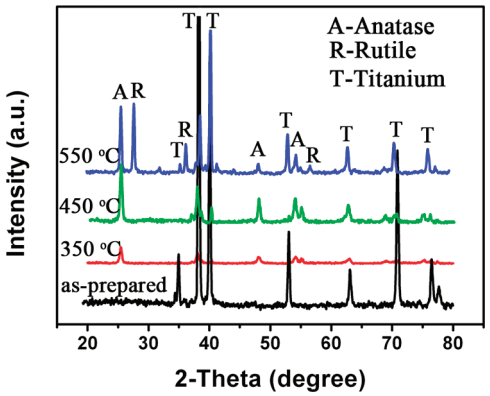

Figure 2. XRD patterns of the TiO_2/Ti mesh electrodes annealed at various temperatures.

calcination temperature increased from 350 to 450 °C, the peak intensity of anatase increased, which is ascribed to the increase in crystallinity and the gradual growth of crystallites. Although the temperature increased to 550 °C, the peaks related to rutile phase start to appear, but most of these phases are still composed of anatase.

3.2. Comparison of Photocatalytic Activity between TiO_2/Ti Mesh and TiO_2/Ti Foil Electrodes. Figure 3 shows the comparison of the photocatalytic activity of the TiO_2/Ti mesh and foil electrodes by degradation of MO solution under the same experimental conditions. If one directly compared the degradation efficiency, a degradation efficiency of 47% is achieved by the TiO_2/Ti mesh electrode compared to 65% by the TiO_2/Ti foil electrode after 360 min of illumination (Figure 3a). That is, when the foil is replaced by the mesh, a decrease is noted from 65 to 47% for the absolute degradation efficiency. The decrease in degradation efficiency might be ascribed to shorter nanotubes on TiO_2/Ti mesh, making its smaller surface area for photocatalytic reaction. However, it is not reasonable to directly compare the absolute degradation efficiency, which cannot be straightly associated with the photocatalytic activity because of the large empty area on Ti mesh. And the TiO_2/Ti foil weighs 0.4 g, whereas TiO_2/Ti mesh with the same apparent area weighs only 0.2 g. Therefore, for comparing the photoactivity of the nanotubes formed over Ti foils and meshes more reasonably, the degradation efficiency is normalized with respect to the mass (Figure 3b). The corresponding values are 214%/g and 176%/g for the TiO_2/Ti mesh and the TiO_2/Ti foil, respectively. About 22% improvement is achieved when the TiO_2/Ti mesh electrode is used. From the view of the practical application, such a lightweight electrode has an advantage in photoreactor design.

In a related work, Kar et al. gave a comparison of the photocatalytic activity of nanotubes formed over the foil and the wire, and the photocatalytic degradation of MO solution was normalized to the total surface area of Ti wire.[17] However, in our case, only one-half of the mesh lateral area could be illuminated directly by the UV light. The other half of the mesh has no significant contribution to the photocatalytic activity. Thus we calculated the degradation rate using the real surface area of the Ti mesh (Figure 3c). The corresponding values are 22%/cm^2 and 16%/cm^2 for the TiO_2/Ti mesh and the TiO_2/Ti foil, respectively. About 38% improvement is achieved in the presence of the TiO_2/Ti mesh.

For the same mass or surface area of illumination, TiO_2 nanotubes formed on Ti mesh are more effective for dye degradation compared to those on Ti foil. We contribute such enhancement of photocatalytic activity to the particular geometry of the TiO_2/Ti mesh electrode as follows. First, the absorbance of scattered radiation is more efficient using the TiO_2 nanotubes formed over the mesh. Unlike planar Ti foil where nanotubes are grown vertically in 2D arrays, the TiO_2/Ti mesh electrode consist of nanotubes that extend radically in a 3D array on a grid of Ti wires. Thus loss of photons attributed to scattering effects in the liquid can potentially be minimized since the nanotubes can absorb reflected and/or refracted light. Figure 3d shows a schematical representation of the benefits of the TiO_2 nanotubes formed over Ti mesh. Moreover, interstitial fissures between the nanotubes allow dye molecules more easily to access the photocatalyst surface, which contributes to the photocatalytic activity as well.

To further understand the improvement of photocatalytic activity using TiO_2/Ti mesh electrodes, the transient photocurrent responses of the TiO_2/Ti mesh and foil electrodes were measured by several on−off cycles of intermittent UV irradiation. Figure 4 shows a comparison of I−t curves of the two electrodes. For both electrodes, the photocurrent value rapidly decreases to zero as soon as the irradiation turns off, and the photocurrent comes back to a constant value when the light turns on again, which shows a good reproducibility. Similar to the comparison of MO degradation efficiency, the photocurrent is also normalized with respect to the mass and surface area, respectively. It can be seen that the photocurrent of the TiO_2/Ti mesh is much larger than that of TiO_2/Ti foil. Higher photocurrent means lower recombination of photogenerated electrons and holes, higher photoelectron transfer efficiency, and/or more light absorbance for TiO_2/Ti mesh electrode, which will eventually benefit the corresponding photocatalysis.[19] Essentially, photocatalysis is a series of reductive and oxidative reactions on photon activated surface. Therefore, to some extent, higher photocurrent also means improved redox properties or photocatalytic activity.[17] The experimental results highly agree with the photocatalytic MO degradation results above, further suggesting the advantages of the mesh-shaped geometry on improving photocatalytic activity.

3.3. MO Degradation by TiO_2/Ti Mesh Electrodes. *3.3.1. Effect of Calcination Temperature.* Figure 5 shows the effect of the calcination temperature of the TiO_2/Ti

dx.doi.org/10.1021/am201220e | ACS Appl. Mater. Interfaces 2012, 4, 171−177

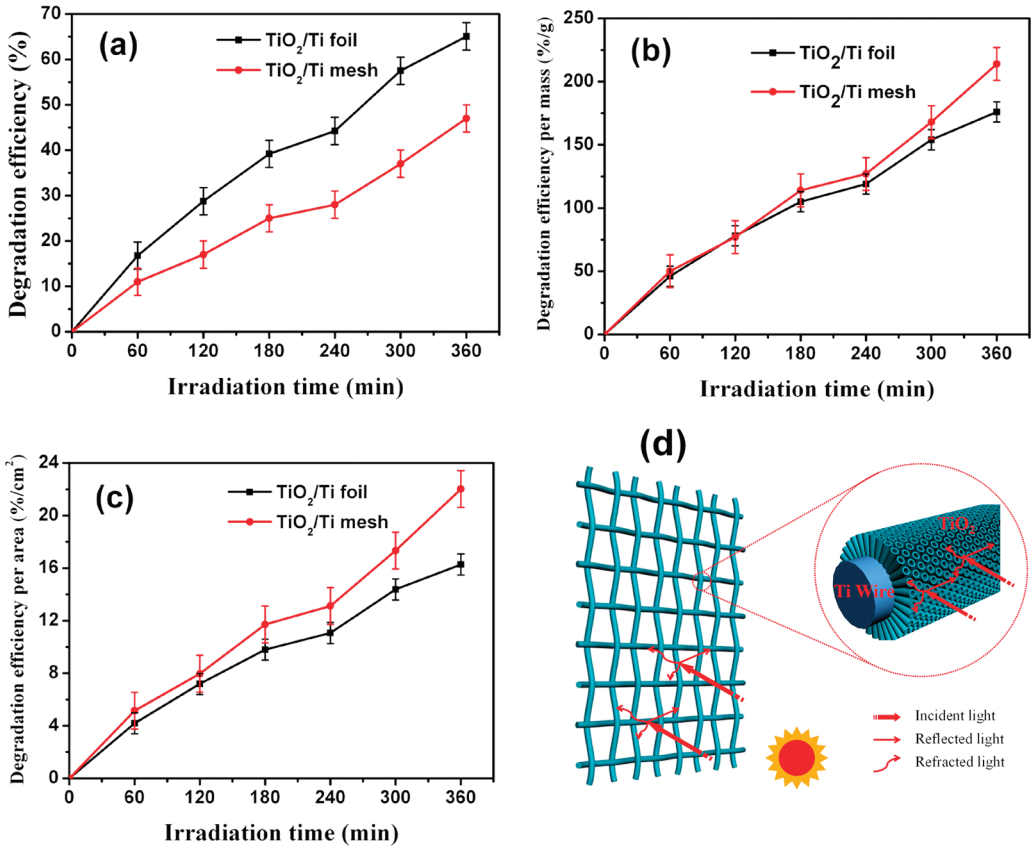

Figure 3. Comparison of the photocatalytic activity of TiO_2/Ti mesh and TiO_2/Ti foil electrodes: (a) absolute degradation efficiency without any normalization; the degradation efficiency is normalized with respect to (b) the mass and (c) the real surface area, respectively. (d) schematical representation of the improvement in the photoactivity of the TiO_2 nanotubes formed on Ti mesh because of the ability to absorb reflected and refracted light.

mesh electrodes on the photocatalytic activity. The photocatalytic activity increases with increasing calcination temperatures from 350 to 550 °C. The electrode calcined at 350 °C shows the lowest photocatalytic activity in the decomposition of MO because of its unsufficient crystallinity. The enhancement of photocatalytic activity with increasing calcination temperatures from 350 to 450 °C can be ascribed to an improvement in the crystallinity of anatase. And the maximal photocatalytic activity was achieved by the TiO_2/Ti mesh electrode calcined at 550 °C. However, our finding is contradicted with the fact that the photocatalytic activity decreased with the increasing calcination temperature due to the sharp drop of the specific surface area after thermal treatment at higher temperature.[20,21] Thus, the contribution by mixed crystal effect can not be ignored. That the TiO_2/Ti mesh electrode calcined at 550 °C has the highest photocatalytic activity can be ascribed to the mixed crystal effect because of the energy band match between anatase and rutile crystals. The photogenerated electrons on the conduction band (CB) of anatase could be injected to the CB of rutile nearby and the photogenerated holes on the valence band (VB) of rutile injected to the VB of anatase, which improved the charge separation and led to an improved photocatalytic activity.[22]

3.3.2. Effect of pH Values in the MO Initial Solution. The wastewater from textile industries usually has a wide range of pH values. Since photocatalysis is a surface reaction, the photocatalyst performance can be highly predisposed by the pH of textile wastewater, the type of the dye, and the ability to be absorbed onto the photocatalyst surface. The pH-value dependence can be explained on the basis of the TiO_2 zero-point charge (zpc). The pH_{zpc} of TiO_2 is widely reported between 6 and 7.[23] In acidic or caustic conditions, the surface of TiO_2 can respectively become positively or negatively charged. For pH values less than pH_{zpc} the surface becomes positively charged, and for pH values greater than pH_{zpc} the TiO_2 surface will be negatively charged, as shown in the following equations[24]

$$TiOH + H^+ \rightarrow TiOH_2^+ \quad (2)$$

$$TiOH + OH^- \rightarrow TiO^- + H_2O \quad (3)$$

Figure 6 shows the effect of initial solution pH values on the MO degradation efficiency. The degradation rates at pH 1, 7, and 13 are 70, 47, and 62%, respectively. These data indicate that the decomposition of MO molecules is easier and quicker under both strong acidic and alkaline conditions. MO molecules are known to be anionic in nature.[25,26] Under acidic condition, the color of MO solution changes from yellow to red and the absorbance peak shifts from 466 to 508 nm (see Figure S4 in the Supporting Information). An increase in degradation efficiency, for pH < pH_{zpc}, can be ascribed to a positively charged photocatalyst surface being more available for the absorption of the MO molecules. In addition, MO molecule structure would be changed mostly into the quinone structure under acidic conditions, and the quinone structure is more prone to oxidation over the azo structure due to the sulfonic groups ($-SO_3^-$) aiding in capturing hydrogen protons and further enhancing the hydrophobicity of the TiO_2 surface.[26]

dx.doi.org/10.1021/am201220e | ACS Appl. Mater. Interfaces 2012, 4, 171–177

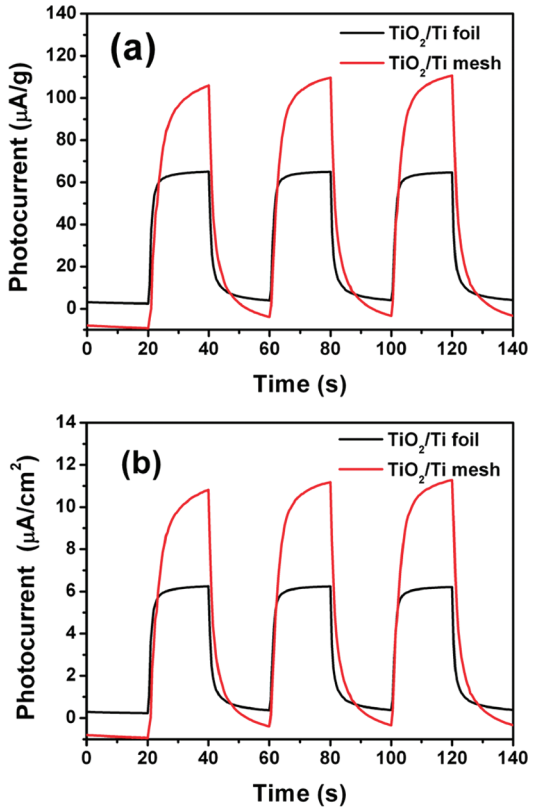

Figure 4. Comparison of photocurrent response of TiO_2/Ti mesh and TiO_2/Ti foil electrodes in 1 M KOH solution: photocurrent is normalized with respect to the (a) mass and (b) surface area, respectively.

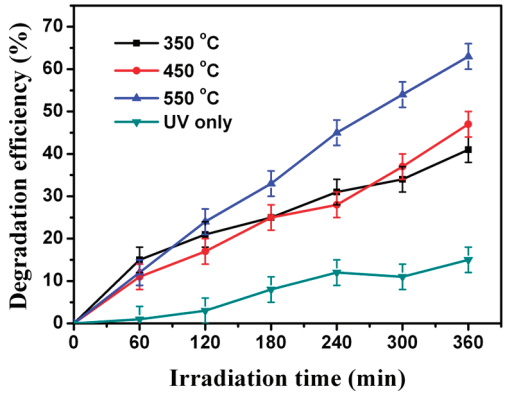

Figure 5. Effect of the calcination temperature on photocatalytic degradation of MO solution.

When pH value is 4, the weak acidity of MO aqueous solution could not make for producing quinone structure. Oppositely, hydrogen ions are propitious to reacting with OH· and weaken the photocatalytic performance. Thereby the degradation rate at pH 1 is maximal in all the degradation reactions. Under alkaline condition, the color of MO solution keeps yellow and the absorbance peak keeps 466 nm (see Figure S4 in the Supporting Information). when pH 10, the MO molecules are difficult to be absorbed onto the TiO_2 surface because of electrostatic repulsion, so the degradation rate decreases with the increase of pH values. However, when pH value rises to be 13, the degradation efficiency increases again. The increase in degradation efficiency with the pH value can be explained in

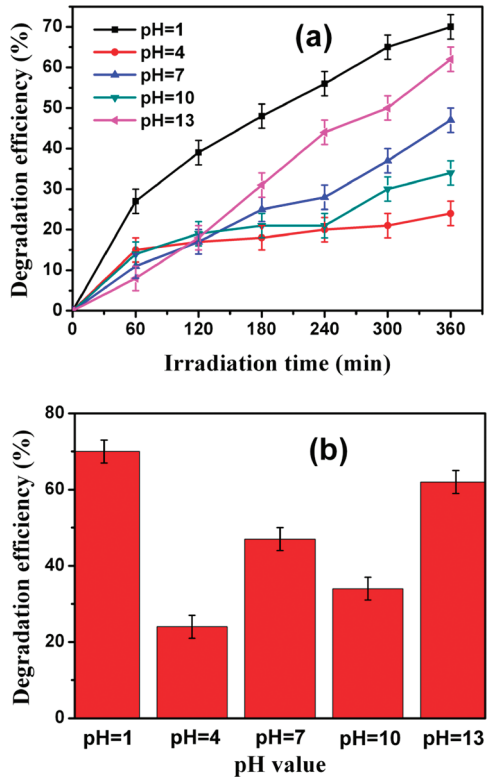

Figure 6. (a) Effect of initial solution pH value on degradation efficiency of MO solution, (b) corresponding columnar section.

that the hydroxyl radicals might be scavenged more rapidly at a higher pH and are allowed them to react more readily with the dye.[26] Thereby, a high degradation efficiency can also be achieved at pH 13.

3.3.3. Effect of Addition of H_2O_2. Moreover, in photocatalytic reactions, the presence of H_2O_2 is considered advantageous since it increases the formation rate of hydroxyl radical by acting as an electron donor, by reduction of H_2O_2 at the conduction band and via self-decomposition by UV light illumination, as described in following equation[27,28]

$$TiO_2 + h\nu \rightarrow h^+ + e^- \quad (4)$$

$$H_2O_2 + e^- \rightarrow OH^- + OH\bullet \quad (5)$$

$$H_2O_2 + h\nu \leftrightarrow 2OH\bullet \quad (6)$$

Therefore, we further investigated the effect of the addition of H_2O_2 (0.3 mM) on the photocatalytic oxidation, as shown in Figure 7. The MO degradation efficiency by the TiO_2/Ti mesh electrode under UV irradiation with H_2O_2 addition (indicated as UV/H_2O_2/ TiO_2–Ti mesh in Figure 7) is 89% after 360 min, while the efficiencies by UV/TiO_2–Ti mesh and UV/H_2O_2 are 47 and 41%, respectively. The MO degradation efficiency by UV/H_2O_2/ TiO_2–Ti mesh system is almost the sum of the individual contributions from the UV/H_2O_2 and UV/TiO_2–Ti mesh systems, respectively. It is interesting to find that when the MO solution was irradiated in the presence of H_2O_2 but without any catalyst, the degradation rate could still reach 41%. This is because UV/H_2O_2 itself is an effective advanced oxidation system for water purification. Under UV irradiation, H_2O_2 will be photolyzed to form two hydroxyl radicals according to eq 5, which could then lead to oxidative degradation of organic molecules. Therefore, the addition of

dx.doi.org/10.1021/am201220e | ACS Appl. Mater. Interfaces 2012, 4, 171–177

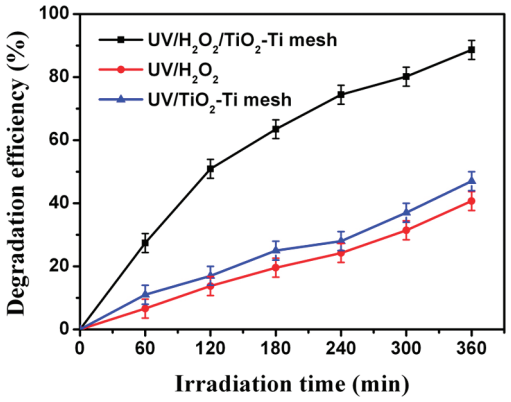

Figure 7. Effect of addition of H_2O_2 on MO degradation under UV irradiation. UV/H_2O_2/ TiO_2−Ti mesh indicates MO degradation by the TiO_2/Ti mesh electrode under UV irradiation with H_2O_2 addition; UV/TiO_2−Ti mesh indicates MO degradation by the TiO_2/Ti mesh electrode under UV irradiation without H_2O_2 addition; UV/H_2O_2 indicates MO degradation under UV irradiation with H_2O_2 addition only.

hydrogen peroxide appears to act synergistically to MO photocatalytic degradation. It can thus be demonstrated that H_2O_2 is able to considerably promote the efficiency of MO photocatalytic degradation by TiO_2/Ti mesh.

3.4. Stability of TiO_2/Ti Mesh Electrodes. To examine the stability of the TiO_2/Ti mesh electrodes, we investigated the photocatalytic degradation ability of the electrode by repeating MO photocatalytic degradation experiments for five times. After each cycle, the TiO_2/Ti mesh was washed thoroughly with water, and a fresh solution of MO was added before each photocatalytic run in the reactor. Figure 8

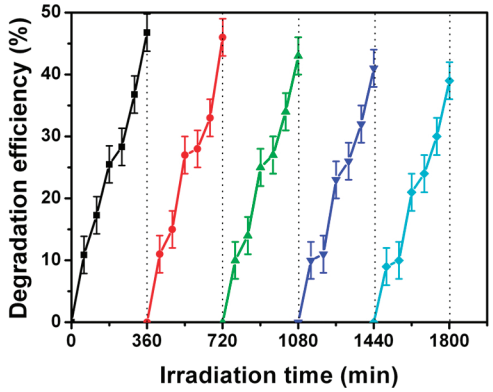

Figure 8. MO photocatalytic degradation by TiO_2/Ti mesh electrodes five times.

indicates that the degradation efficiency is very stable with only a little decrease of about 8% at the fifth cycle. This suggests that TiO_2/Ti mesh electrode processes excellent stability and reliability for photocatalysis of pollutants.

For such a TiO_2/Ti mesh photoelectrode, there should exist an optimal geometric mesh structure, where mesh number, wire diameter, nanotube length and diameter, etc. can be further optimized, leading to more effective absorption of the incident light and even superior photocatalytic efficiency. For example, for a series of Ti meshes with the same wire diameter, increasing the mesh number (that is, the increase in the number of wires) should improve the photocatalytic efficiency since a larger surface area can be available for producing nanotube arrays and absorbing dye molecules. Further experimental as well as theoretical studies are required to clarify the relationship between the structure and photocatalytic properties, which could not only provide important insight into the understanding of the underlying mechanism but also have implications to the optimization of the photocatalytic reactors.

4. CONCLUSIONS

In summary, we have successfully fabricated a new type of TiO_2/Ti mesh photoelectrode by anodization in ethylene glycol solution. Compared with the TiO_2/Ti foil electrode, the mesh electrode possesses a 3D TiO_2 nanotube arrays and behaves with high efficiency in degrading methyl orange. The corresponding degradation efficiency can reach 22 and 38% enhancement in per mass and per area, respectively. The enhanced photocatalytic activity can be ascribed to the improved light absorbance by the nanotubes formed over Ti mesh. Furthermore, it has been found that the calcination temperature, initial solution pH values and the addition of H_2O_2 can significantly influence the MO degradation efficiency. According to the effect of crystal structures, the maximum of photocatalytic activity is observed at 550 °C due to the appearance of mixed crystal phases of anatase and rutile. In strong acidic or caustic conditions, such as pH 1 and 13, a high degradation efficiency can be both achieved. The presence of H_2O_2 in photocatalytic reactions can promote photocatalytic degradation efficiencies. These results demonstrate the importance of choosing the optimum photodegradation parameters to obtain high degradation efficiency, which is essential for practical application of the process. More importantly, the TiO_2/Ti mesh electrode shows great stability in repeated MO degradation, which can benefit its potential applications in solar energy conversion and wastewater purification.

■ ASSOCIATED CONTENT

Ⓢ Supporting Information

Schematic diagrams of 3D and 2D arrays of TiO_2 nanotubes, SEM images and XRD patterns of TiO_2/Ti foil electrodes, UV−vis absorption spectroscopy of MO degradation at pH 1, pH 7, and pH 13. This material is available free of charge via the Internet at http://pubs.acs.org.

■ AUTHOR INFORMATION

Corresponding Author

*Tel./Fax: +86 898 66276115. E-mail: swlin77@gmail.com.

■ ACKNOWLEDGMENTS

This work was supported by Program for New Century Excellent Talents in University (NCET-09-0110), the Key Project of Chinese Ministry of Education (210171), Hainan Natural Science Foundation (511110), and the Scientific Research Foundation for the Returned Overseas Chinese Scholars, State Education Ministry. We acknowledge Mr. Guizhen Wang for the analysis of scanning electron microscopy in the Analytical and Testing Center of Hainan University.

■ REFERENCES

(1) Chen, D. W.; Ray, A. K. *Appl. Catal., B: Environ.* **1999**, *23*, 143−157.
(2) Zhou, H.; Smith, D. W. *J. Environ. Engin. Sci.* **2002**, *1*, 247−264.

(3) Chong, M. N.; Jin, B.; Chow, C. W. K.; Saint, C. *Water Res.* **2010**, *44*, 2997−3027.
(4) Butterfield, I. M.; Christensen, P. A.; Hamnett, A.; Shaw, K. E.; Walker, G. M.; Walker, S. A.; Howarth, C. R. *J. Appl. Electrochem.* **1997**, *27*, 385−395.
(5) Bianco, Prevot A.; Baiocchi, C.; Brussino, M. C.; Pramauro, E.; Savarino, P.; Augugliaro, V.; Marcì, G.; Palmisano, L. *Environ. Sci. Technol.* **2001**, *35*, 971−976.
(6) Comparelli, R.; Fanizza, E.; Curri, M. L.; Cozzoli, P. D.; Mascolo, G.; Passino, R.; Agostiano, A. *Appl. Catal., B: Environ.* **2005**, *55*, 81−91.
(7) Wender, H.; Feil, A. F.; Diaz, L. B.; Ribeiro, C. S.; Machado, G. J.; Migowski, P.; Weibel, D. E.; Dupont, J.; Teixeira, S. R. *ACS Appl. Mater. Interfaces* **2011**, *3*, l359−1365.
(8) Byrne, J. A.; Eggins, B. R.; Brown, N. M. D.; McKinney, B.; Rouse, M. *Appl. Catal., B: Environ.* **1998**, *17*, 25−36.
(9) Pecchi, G.; Reyes, P.; Sanhueza, P.; Villaseňor, J. *Chemosphere* **2001**, *43*, 141−146.
(10) Wu, N. L.; Lee, M. S.; Pon, Z. J.; Hsu, J. Z. *J. Photochem. Photobiol., A* **2004**, *163*, 277−280.
(11) Costacurta, S.; Maso, G. D.; Gallo, R.; Guglielmi, M.; Brusatin, G.; Falcaro, P. *ACS Appl. Mater. Interfaces* **2010**, *2*, 1294−1298.
(12) Grimes, C. A.; Mor, G. K. *Optical & Electronic Materials*; Springer: New York, 2009; p 5.
(13) Paulose, M.; Prakasam, H. E.; Varghese, O. K.; Peng, L.; Popat, K. C.; Mor, G. K.; Desai, T. A.; Grimes, C. A. *J. Phys. Chem. C* **2007**, *111*, 4992−14997.
(14) Zhuang, H. F.; Lin, C. J.; Lai, Y. K.; Sun, L.; Li, J. *Environ. Sci. Technol.* **2007**, *41*, 4735−4740.
(15) Beranek, R.; Macak, J. M.; Gätner, M.; Meyer, K.; Schmuki, P. *Electrochim. Acta* **2009**, *54*, 2640−2646.
(16) Liu, Z. Y.; Subramania, V.; Misra, M. *J. Phys. Chem. C* **2009**, *113*, 14028−14033.
(17) Kar, A.; Smith, Y. R.; Subramanian, V. *Environ. Sci. Technol.* **2009**, *43*, 3260−3265.
(18) Frandsen, C. J.; Jin, S.; Tauber, M. J. *J. Phys. Chem. B* **2010**, *114*, 14537−14543.
(19) Xie, Y. B. *Adv. Funct. Mater.* **2006**, *16*, 1823−1831.
(20) Ding, Z.; Lu, G. Q.; Greenfield, P. F. *J. Phys. Chem. B* **2000**, *104*, 4815−4820.
(21) Peng, T. Y.; Zhao, D.; Dai, K.; Shi, W.; Hirao, K. *J. Phys. Chem. B* **2005**, *109*, 4947−4952.
(22) Mu, Q. H.; Li, Y.; Zhang, Q. H.; Wang, H. Z. *J. Hazard. Mater.* **2011**, *188*, 363−368.
(23) O'Shea, K. E.; Pernas, E.; Saiers, J. *Langmuir* **1999**, *15*, 2071−2076.
(24) Sun, J. H.; Qiao, L. P.; Sun, S. P.; Wang, G. L. *J. Hazard. Mater.* **2008**, *155*, 312−319.
(25) Gehlen, M. H.; Ferreira, M.; Neumann, M. G. *J. Photochem. Photobiol., A* **1995**, *87*, 55−60.
(26) Smith, Y. R.; Kar, A.; Subramanian, V. *Ind. Eng. Chem. Res.* **2009**, *48*, 10268−10276.
(27) Coleman, H. M.; Vimonses, V.; Leslie, G.; Amal, R. *J. Hazard. Mater.* **2007**, *146*, 496−501.
(28) Silva, A. M. T.; Nouli, E.; Xekoukoulotakis, N. P.; Mantzavinos, D. *Appl. Catal., B: Environ.* **2007**, *73*, 11−22.